



## EFFECT OF THE PROCESSING METHODS ON THE FORMATION OF $Al_3C_2$ IN $SiC_p/2024$ Al COMPOSITES

Don-Soo Shin<sup>1</sup>, Jae-Chul Lee<sup>2\*</sup>, Eui-Pak Yoon<sup>3</sup> and Ho-In Lee<sup>2</sup>

<sup>1</sup>Sam Sun Industrial Co., Ltd, 345-11, Gasan, Kumchon, Seoul, Korea

<sup>2</sup>Division of Metals, Korea Institute of Science and Technology  
P.O. Box 131 Cheongryang, Seoul 130-650, Korea

<sup>3</sup>Department of Metallurgical Engineering, Hanyang University,  
Hangdang, Seongdong, Seoul, Korea

(Refereed)

(Received October 31, 1996; Accepted November 8, 1996)

### ABSTRACT

$SiC_p/2024$  Al composites were prepared using various processing techniques, such as the spray forming, thixoforming, and compocasting. The interfacial characterizations of these composites were performed using scanning electron microscopy, Auger electron spectrometry, transmission electron microscopy, and X-ray diffraction on reaction products extracted by the electrochemical dissolution. The value of these combined techniques in elucidating the morphologies of the interfacial reaction products was also demonstrated. The influence that each fabrication process has on the extent of the interfacial reaction was studied. © 1997 Elsevier Science Ltd

**KEYWORDS:** A. carbides, A. composites, A. interfaces, C. differential scanning calorimetry (DSC), and C. X-ray diffraction

### INTRODUCTION

Improved mechanical properties of Al alloy composites reinforced with  $SiC$  particulates ( $SiC_p$ ) are due to the transfer of shear load at the matrix/reinforcement interface. As a result, composite interfaces play important roles in determining the resultant composite properties.

\*To whom correspondence should be addressed.

According to the various theoretical and experimental studies, SiC reacts with Al to form  $Al_4C_3$  and Si according to the reaction.



This reaction is known to have several undesirable effects on the overall composite properties: (i) The interfacial reaction product  $Al_4C_3$  degrades the mechanical and physical properties of the reinforcement. (ii) Since the reaction product  $Al_4C_3$  is unstable in some environments such as water, methanol, and HCl [1,2], the composite can be susceptible to corrosive environments. (iii) In addition, silicon, formed as an interfacial reaction product, produces the Al–Si eutectic at the interface and the grain boundary regions, resulting in undesired mechanical properties of the composite. Consequently, fabrication of SiC/Al composite devoid of  $Al_4C_3$  has been a major goal. Among the various methods proven to be effective in achieving such a goal, two methods have been widely accepted: addition of Si into Al matrix [3–6] and artificial oxidation of SiC to produce  $SiO_2$  layer on the surface of SiC [6–8]. However, considering that the reaction given by eq. 1 is dependent on temperature and holding time, processing methods also affect the extent of the interfacial reaction.

SiC<sub>p</sub>/Al alloy composites devoid of the hazardous interfacial reaction products can be fabricated by using adequate processing techniques. The purpose of the present study was to investigate the influence that various fabrication techniques have on the extent of the interfacial reaction in the SiC<sub>p</sub>/2024 Al composite.

## EXPERIMENTAL PROCEDURES

**Composite Fabrication.** SiC<sub>p</sub>/2024 Al composites used in this study were fabricated using three different processing routes, namely, spray forming, thixoforming, and compocasting routes. SiC<sub>p</sub> used as the reinforcement were mostly  $\alpha$ -SiC (6H) mixed with a small amount of  $\beta$ -SiC (3C) and the average size of SiC<sub>p</sub> was 25  $\mu$ m. The chemical composition of 2024 Al alloy is shown in Table 1.

15 vol% SiC<sub>p</sub>/2024 Al composite billet, with dimensions of  $\Phi 250 \times 1000$  mm, was fabricated using a spray forming process in nitrogen atmosphere. The as-fabricated composite billet was then hot extruded at 450°C with an extrusion ratio of 27:1, to eliminate porosity formed during the fabrication stage. Thixoforming was used to form a composite plate. The spray-formed composite was used as the raw material for thixoforming. Before applying the required force for thixoforming, the spray-formed composite billet was heated to a semi-solid region (630°C for 10 min). The heated slug was then injected into the mold to form a composite plate using a 250 ton hydraulic press. In the case of the compocasting, 15 vol% of SiC<sub>p</sub> were added into the molten 2024 Al alloy, which was held at a temperature

TABLE 1  
Chemical Composition of 2024 Al Used for the Study

| Matrix alloy | Wt.% of alloying elements |      |      |      |      |      |      |      |     |
|--------------|---------------------------|------|------|------|------|------|------|------|-----|
|              | Mg                        | Si   | Cu   | Fe   | Cr   | Mn   | Zn   | Ti   | Al  |
| 2024 Al      | 0.48                      | 0.72 | 4.21 | 0.10 | 0.01 | 0.80 | 0.07 | 0.01 | Rem |

TABLE 2  
Summary of the Processing Conditions Used for Composite Fabrication

|                  | Spray forming  | Thixoforming | Compoasting  |
|------------------|----------------|--------------|--------------|
| Fab. temperature | 560 °C         | 630 °C       | 700 → 640 °C |
| Holding time     | 5–15 min       | 10 min       | 60 min       |
| Fab. atmosphere  | N <sub>2</sub> | Air          | Air          |

of 700°C. The mixture of the molten Al alloy and SiC<sub>p</sub> was then continuously stirred from 700 to 640°C with a ceramic stirrer to promote uniform distribution of SiC<sub>p</sub> within the matrix alloy and poured into a mold. Processing conditions used for this study are summarized in Table 2.

**Analyses.** When the size and volume fraction of the interfacial reaction products within the composites are relatively small, the resultant X-ray diffraction intensities from these reaction products become weak, making it difficult to determine the exact peak positions required for phase identification. In order to overcome such a problem, SiC<sub>p</sub> and the interfacial reaction products were extracted from the composite using the electrochemical dissolution method [9–11]. The electrolyte used was 33 vol% HNO<sub>3</sub> and 67 vol% water. The voltage and current used for the extraction were 11 DC volts and 6 amp, respectively. The electrolyte was maintained at 20–30°C throughout the extraction procedure. The extracted powders were then coated onto a transparent tape for X-ray diffraction. In order to observe the interfacial reaction products using SEM, the extracted powders were coated with Pt having an approximate thickness of 80 Å to help observe the 3-dimensional morphologies of the interfacial reaction products at high magnifications. Detailed 3-dimensional morphologies of interfacial reaction products at the interface were examined using a Hitachi S-4200 Field Emission scanning electron microscope operated at 15 kV. In order to prepare sound specimens for SEM observations, special care has to be taken to make sure that the interfacial reaction products are not dissolved into the electrolyte during the extraction and that the surface of the sample are not coated with the etching product.

## RESULTS

**Microstructures.** Presented in Figure 1 are optical micrographs showing the distribution of SiC<sub>p</sub> within the composites. In the case of the sprayformed composites, SiC<sub>p</sub> were observed to be distributed uniformly within the matrix. However, SiC<sub>p</sub> within the thixoformed and the compocast composites were found to be segregated at the grain boundary regions. In addition, the Si–CuAl<sub>2</sub> ternary eutectic phase as well as some interfacial reaction products, which were not observed in the sprayformed composites, were observed both at the grain boundary regions and near SiC<sub>p</sub>.

**Observation of the Interfacial Reaction Products.** Observation of detailed 3-dimensional morphologies of the interfacial reaction products, which in general is not possible under TEM, was carried out using SEM. For this purpose, SiC<sub>p</sub> were extracted from the thixoformed SiC<sub>p</sub>/2024 Al composite using the electrochemical dissolution method. Figure 2(a) shows SiC<sub>p</sub> on which the interfacial reaction products are attached. Based on XRD results obtained from the extracted powders, the interfacial reaction products observed in

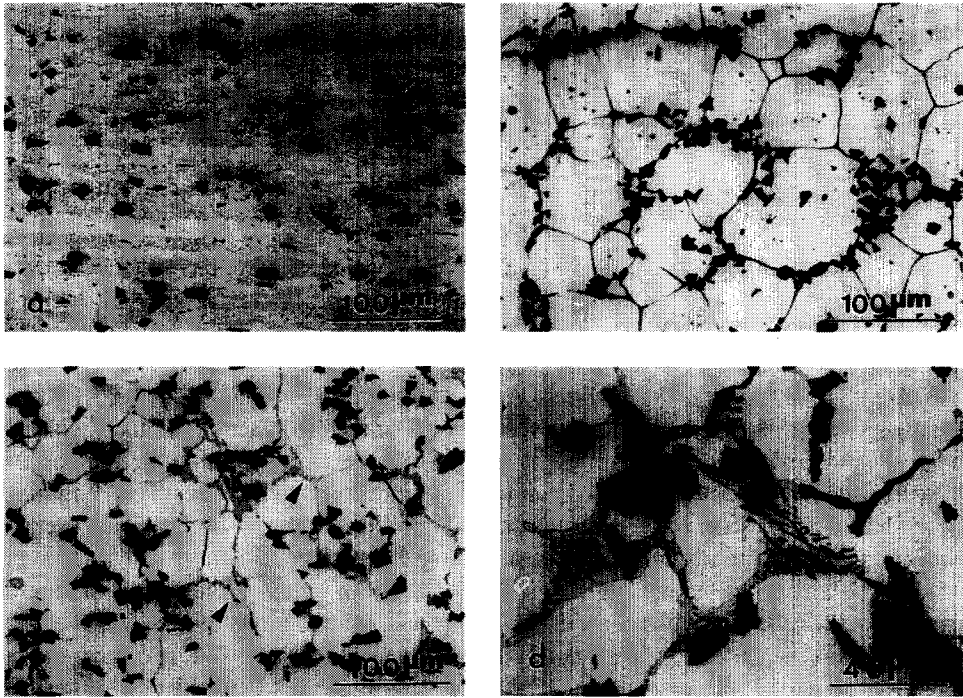


FIG. 1

Optical micrographs showing the distribution of  $\text{SiC}_p$  in the  $\text{SiC}_p/2024$  Al composites fabricated by using (a) sprayforming, (b) thixoforming, and (c) compocasting techniques. Notice the segregation of  $\text{SiC}_p$  and the presence of  $\text{Si-CuAl}_2$  eutectic at the grain boundary regions of the compocast composite, as indicated by the arrows. (D) Magnified view of the compocast composite, showing the reacted  $\text{SiC}_p$  and  $\text{Si-CuAl}_2$  eutectic.

Figure 2(a) were identified as  $\text{Al}_4\text{C}_3$  and Si, as shown in Figure 2(b). Such interfacial reaction products are reported to form as a result of the interfacial reaction given by eq. 1. Detailed morphologies of the reaction products formed at the surface of  $\text{SiC}$  particulate are presented in Figure 3(a). According to the analytical results obtained from the Auger electron analysis carried out on an image similar to Figure 3(a), the thin hexagonal platelets were identified as  $\text{Al}_4\text{C}_3$  and the dendritic-shaped crystals were Si.

**Effect of Processing Methods on the Extents of the Interfacial Reactions.** The amount of the free Si formed as a result of the interfacial reaction increases with increasing temperature and holding time, which in turn results in decrease in the liquidus temperature of the composite. Therefore, measurement of the liquidus temperature can be used as a qualitative means for measuring the extent of the interfacial reactions within the composites. For such purposes, a differential thermal analyzer (DTA), which was calibrated using various pure metals, was used to measure the liquidus temperatures of the composites.

Shown in Figure 4 are DTA traces corresponding to the sprayformed, thixoformed, and compocast composites. In the case of the sprayformed composite, upon heating, stable

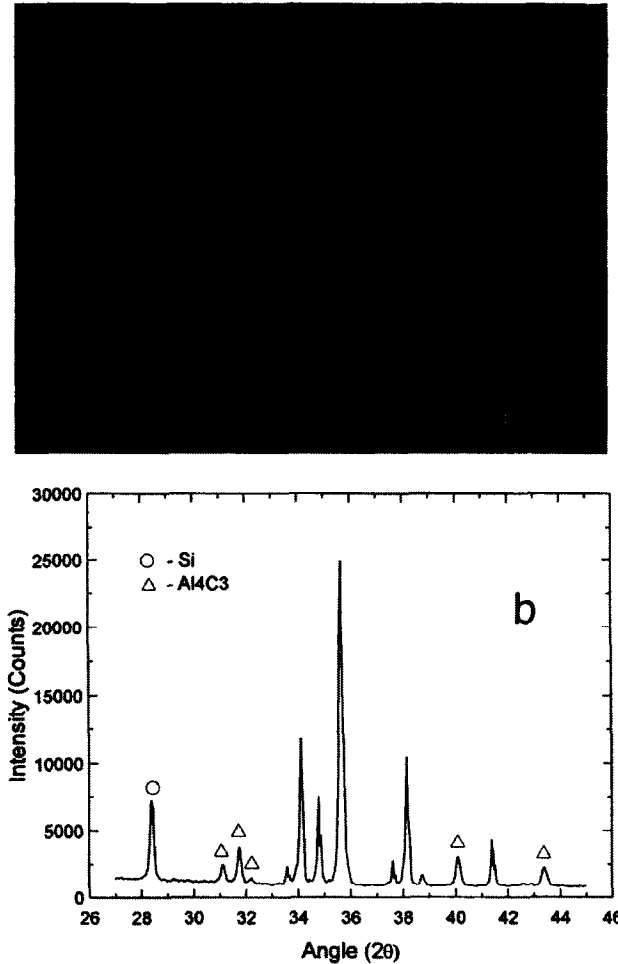


FIG. 2

(a) SEM micrograph of SiC<sub>p</sub>, extracted from the thixoformed SiC<sub>p</sub>/2024 Al composite, which was held at 630°C for 10 min. Presence of various reactions products on the surface of SiC<sub>p</sub> is evident. (b) XRD obtained from the extracted SiC<sub>p</sub>, indicating that interfacial reaction products formed at the reinforcement surface are Al<sub>4</sub>C<sub>3</sub> and Si. The unmarked peaks in the graph are from SiC<sub>p</sub>.

$\alpha + \theta$  (CuAl<sub>2</sub>) phases within the matrix transform into the single  $\alpha$  phase once the temperature reaches above the solvus, resulting in the appearance of a small endothermic peak at approximately 513°C, as indicated by A in Figure 4. With continued heating, a strong endothermic peak appears at around 644°C, indicating the melting of the matrix alloy. In the case of the thixoformed composite, a similar DTA trace to that of the sprayformed composite is observed, except at a slightly lower liquidus temperature. On the other hand, the DTA trace obtained for the comocast composite shows another endothermic peak, associated with the eutectic reaction indicated by B in Figure 4, at approximately 545°C, with an even lower melting point. The lower melting point and the appearance of a peak at 545°C are due to increased Si content within the composite, which was caused by the

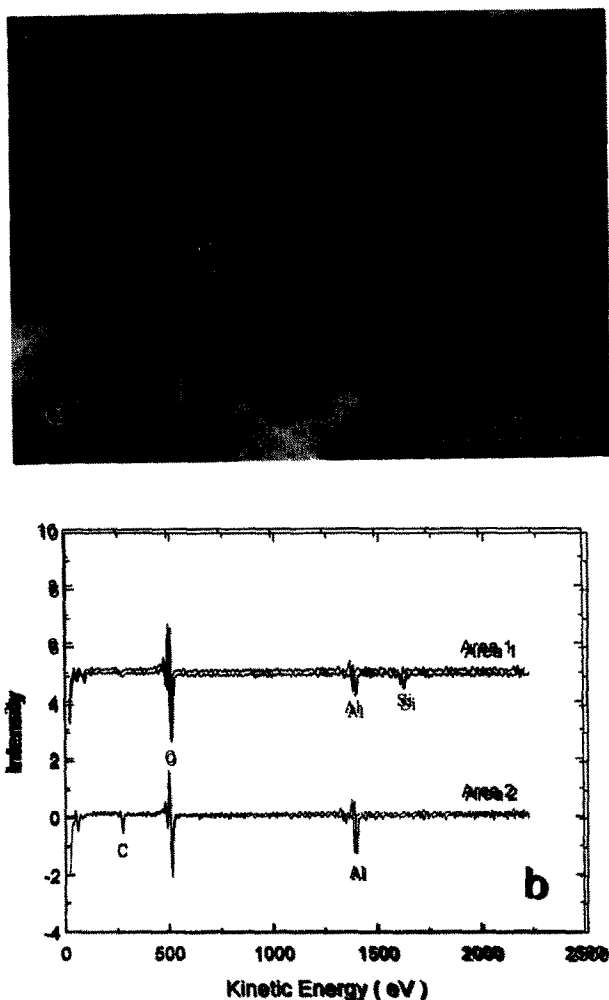


FIG. 3

(a) SEM micrograph showing dendritic-shaped Si crystals (Area 1) and Al<sub>4</sub>C<sub>3</sub> crystals having hexagonal platelet shape (Area 2) similar to that used for Auger electron analysis. (b) Auger electron spectra obtained from the interfacial reactions products.

interfacial reaction given by eq. 1. When the Si content approaches the ternary (Al–Si–Cu) eutectic composition of the matrix alloy, Si along with Al and Cu form eutectic phases, i.e., Si and CuAl<sub>2</sub>, during solidification. CuAl<sub>2</sub> within the eutectic later dissolves during the electrochemical extraction process, leaving a trace of the eutectic Si on the surface of SiC<sub>p</sub>, as seen in Figure 3(a). In addition, Si formed by the eq. 1, which was dissolved into the matrix at the elevated temperature, also forms eutectic phases at the grain boundary regions during solidification.

Direct observations of the extracted powders was carried out using SEM to visualize detailed 3-dimensional morphologies of the interfacial reaction products within the composites. Figure 5 shows surface morphologies of SiC<sub>p</sub> extracted from various composites. As can be seen in these micrographs, SiC<sub>p</sub> extracted from the sprayformed

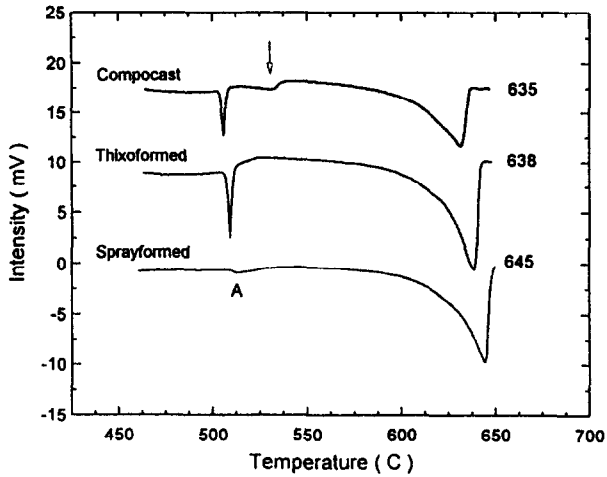


FIG. 4

DTA trace showing the influence of heat treatment temperatures on the formation of Al-Si-Cu eutectic and variation in the melting temperatures in  $\text{SiC}_p/\text{Al}$  composites. The numbers in the graphs indicate the liquidus temperatures of the corresponding composites.

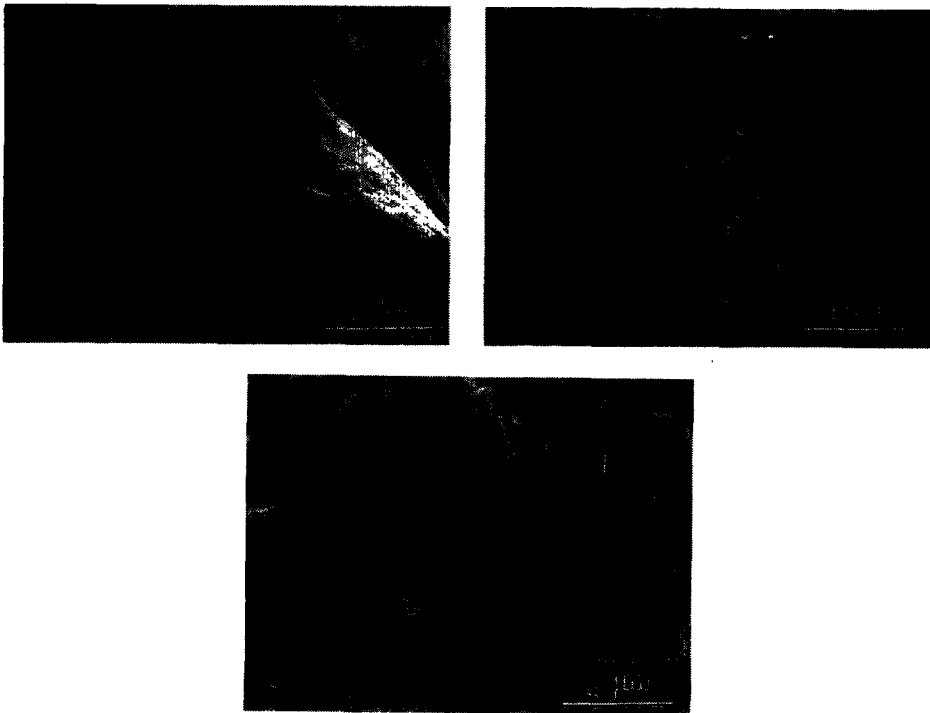


FIG. 5

SEM micrographs showing the surface morphologies of  $\text{SiC}_p$  extracted from (a) the sprayformed composite (560°C for 10 min), (b) thixoformed composite (630°C for 10 min), and (c) compcast composite (700°C for 1 h).

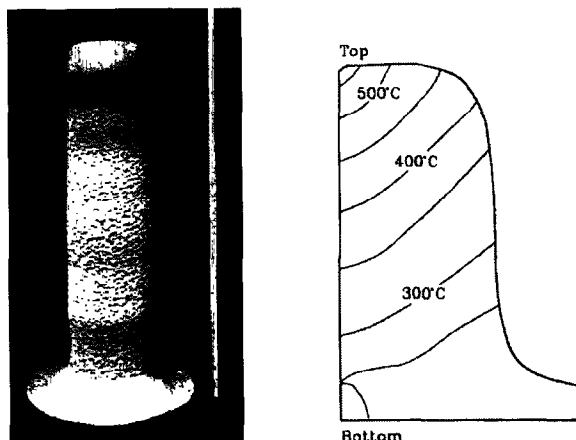


FIG. 6

A sprayformed composite billet. (b) A plot showing the calculated temperature contour within the billet during the fabrication stage. The height of the billet considered in the calculation was 200 mm and the forming speed was 2 cm/min.

composite [Fig. 5(a)] reveals an insignificant amount of reaction products at its surface. However,  $\text{SiC}_p$  extracted from the thixoformed and the compocast composites were covered with a considerable amount of interfacial reaction products, i.e.,  $\text{Al}_4\text{C}_3$  and  $\text{CuAl}_2$ -Si eutectic. Such features are observed in Figures 5(b) and (c). In addition,  $\text{SiC}_p$  extracted from the compocast composite were observed to have severe erosion, as indicated by the arrow in Figure 5(c).

The less severe interfacial reactions in the sprayformed composite are considered to be due to the lower fabrication temperature and shorter holding time of this process. According to the numerical analyses, during spray forming, the maximum temperature of the billet can reach as high as  $560^\circ\text{C}$ . Figures 6(a) and (b) present the as-fabricated composite billet and the calculated temperature contour of the billet during the fabrication stage, showing a gradual decrease in temperature from the top to the bottom of the billet.

## CONCLUSIONS

Hexagonal platelet shaped  $\text{Al}_4\text{C}_3$  and Si are the two major interfacial reaction products of the  $\text{SiC}_p/2024$  Al composite. However, Si later reacts with the matrix alloy to form Si and  $\text{CuAl}_2$  eutectic at the surface of  $\text{SiC}_p$  and at the grain boundary regions. Si and  $\text{CuAl}_2$  crystals were observed in the form of alternating dendritic rods at the SiC/Al interface. Such features of these crystals are due to the results of the ternary eutectic solidification at the presence of enough Si.

The interfacial reactions observed in this composite are dependent on the processing temperature and the holding time. DTA results can be used as an effective tool for the qualitative measurement of the interfacial reactions. Based on the results obtained from DTA and SEM, insignificant amounts of the interfacial reactions were observed to occur in the sprayformed composite. On the other hand, considerable amounts of the interfacial reactions were observed to take place both in the thixoformed and the compocast composites.

## REFERENCES

1. *CRC Handbook of Chemistry and Physics*, 74th ed., pp 4-36, CRC Press (1992).
2. *The Merck Index*, 10th ed., p. 50, Merck (1983).
3. A.C. Ferro and B. Derby, *Acta Metall. Mater.* **43**, 3061 (1995).
4. J.C. Viala, P. Fortier and J. Bouix, *J. Mater. Sci.* **25**, 1842 (1990).
5. J. Narciso, C. Garcia-Cordovilla and E. Louis, *Mater. Sci. Eng.* **B15**, 148 (1992).
6. H. Ribes, M. Suery, G. L'Esperance, and T.G. Legoux, *Mett. Trans. A.* **21**, 2489 (1990).
7. W.M. Zhong, G. L'Esperance, and M. Suery, *Mett. Trans. A.* **26**, 2637 (1995).
8. D.J. Lloyd, H. Lagace, A. Mcleod, and P.L. Morris, *Mat. Sci. Eng.* **A107**, 73 (1989).
9. J.C. Lee, K.N. Subramanian and Y. Kim, *J. Mat. Sci.* **29**, 1983 (1994).
10. J.C. Lee, J.-I. Lee, and H.-I. Lee, *J. Mat. Sci. Lett.* **15**, 1539 (1996).
11. J.C. Lee, J.-I. Lee, and H.-I. Lee, *Scripta Mett.* **35(6)**, 721 (1996).